

Force Analysis of the 6DOF Parallel Manipulators

Yasunobu HITAKA*, Yoshito TANAKA*, Junko ISHII*

*Department of Control and Information Systems Engineering,
Kitakyushu National College of Technology, Japan
E-mail:hitaka@kct.ac.jp

Abstract

The 6DOF (degrees of freedom) Parallel Manipulators have some advantages that are high power, high rigidity, high precision for positioning and compact mechanism compared with conventional serial link manipulators. For these Parallel Manipulators, it can be expected to work in the new fields such that the medical operation, high-precision processing technology and so on. For this expectation, it is necessary to control the action reaction pair of forces which act between the Parallel Manipulator and the operated object. In this paper, we analyze the dynamics of the 6DOF Parallel Manipulator and present numerical simulation results.

1 Introduction

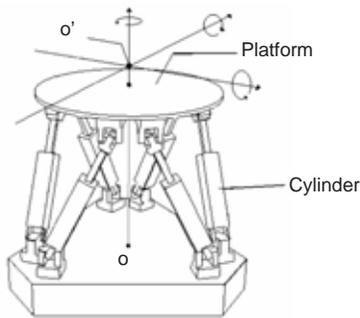


Figure 1: Parallel manipulator

Figure 1 is a type of the parallel manipulators that is called "Stewart Platform"[1]. It consists of a top plate, a bottom plate, and 6 hydraulic cylinders attached to the top and bottom plates. The top plate is called "platform", and the bottom plate is "base". The platform can be achieved six degree of freedom

motion by six cylinders stretching. The character of this manipulator is that the workspace is narrow compared with conventional serial link manipulators. However, Stewart Platform have many redeeming features that are high power, high rigidity, positioning accuracy and compact mechanism. Then, it can be expected to work in the fields which require the operation with high power and high accurate positioning such that the operative treatment, high-precision processing in factory and so on. For these purpose, the force control of this manipulator is necessary but the force analysis for Stewart Platform type of manipulator has never been examined. Thus, we analyze the dynamics of this manipulator.

This paper is consist of 6 sections. This section is introduction. Next section, kinematics of the parallel manipulator is discussed. In 3rd section, we consider the forces which act on the platform. And then, in section 4, we will analyze the dynamics of parallel manipulator. Section 5, we show the numerical simulation results and summary is in section 6.

2 Kinematics of the parallel manipulator [2]

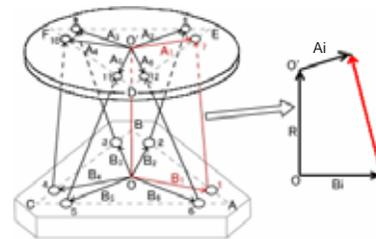


Figure 2: Vector diagram of the parallel manipulator

Figure 2 is a relationship diagram for the vectors of the parallel manipulator. This manipulator has two

reference frame. The one is the motion frame and the other is the base fixed frame. The motion frame is located at the centroid o' of the platform, while the base fixed frame has its origin at the centroid o of the base of the manipulator. The attitude of the platform is specified by the orientation of the motion frame and the position of the centroid o' is located with respect to the base fixed frame.

The right part of Figure 2 focuses the vectors related to the i -th cylinder ($i=1,\dots,6$). The position of the centroid o' is represented by vector $\mathbf{R} = (x, y, z)^T$ with respect to the base fixed frame. The vector \mathbf{A}_i denotes the attachment point of the cylinder on the platform and the vector \mathbf{B}_i denotes attachment point on the base of the manipulator with respect to the base fixed frame. Then, the cylinder length vector \mathbf{l}_i can be calculated by

$$\mathbf{l}_i = \mathbf{A}_{im} \mathbf{T} + \mathbf{R} - \mathbf{B}_i, \quad (1)$$

where \mathbf{A}_{im} describes the attachment point of the cylinder on the platform relative to the motion frame and \mathbf{T} is the oriental matrix of the platform which can be represented by

$$\mathbf{T} = \begin{bmatrix} 1 & 0 & 0 \\ 0 & \cos \phi & \sin \phi \\ 0 & -\sin \phi & \cos \phi \end{bmatrix} \\ \times \begin{bmatrix} \cos \theta & 0 & -\sin \theta \\ 0 & 1 & 0 \\ \sin \theta & 0 & \cos \theta \end{bmatrix} \begin{bmatrix} \cos \psi & \sin \psi & 0 \\ -\sin \psi & \cos \psi & 0 \\ 0 & 0 & 1 \end{bmatrix}. \quad (2)$$

with roll-pitch-yaw angles as ϕ , θ and ψ .

3 The forces act on the platform

Figure 3 is the force analytical model of the parallel manipulator. As shown this diagram, the platform are acted three types of force: the cylinder force $\mathbf{F}_i (i = 1, \dots, 6)$, an external force \mathbf{L} and gravity force \mathbf{M} . We consider these force vectors having coordinates $(F_{ix}, F_{iy}, F_{iz}, i = 1, \dots, 6)$, (L_x, L_y, L_z) and $(0, 0, -mg)$ with respect to the base fixed frame, respectively. Where m is the mass of the platform and g is the gravity acceleration.

If the motion frame and base fixed frame are expressed by $(\mathbf{i}, \mathbf{j}, \mathbf{k})^T$ and $(\mathbf{e}_1, \mathbf{e}_2, \mathbf{e}_3)^T$, respectively, the relations among two frames can be described as $(\mathbf{i}, \mathbf{j}, \mathbf{k})^T = \mathbf{T}(\mathbf{e}_1, \mathbf{e}_2, \mathbf{e}_3)^T$ or $(\mathbf{e}_1, \mathbf{e}_2, \mathbf{e}_3)^T = \mathbf{T}^T(\mathbf{i}, \mathbf{j}, \mathbf{k})^T$. Where $\mathbf{T}^T = \mathbf{T}^{-1}$ is given because the oriental matrix \mathbf{T} is the orthogonal transformation

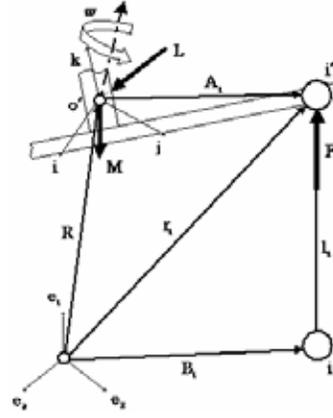


Figure 3: Analytical model of parallel manipulator

matrix. Then, for the cylinder force \mathbf{F}_i , the following relationships

$$\begin{aligned} (F_{ix}, F_{iy}, F_{iz}) &= (F_{i1}, F_{i2}, F_{i3}) \mathbf{T} \\ (F_{i1}, F_{i2}, F_{i3}) &= (F_{ix}, F_{iy}, F_{iz}) \mathbf{T}^T \end{aligned} \quad (3)$$

can be obtained, where (F_{i1}, F_{i2}, F_{i3}) is a coordinate of the vector \mathbf{F}_i with respect to the motion frame.

Furthermore, when the coordinate of i -th cylinder vector \mathbf{l}_i is represented by (l_{ix}, l_{iy}, l_{iz}) with respect to the base fixed frame, we obtain a relation

$$(F_{ix}, F_{iy}, F_{iz}) = \frac{\mathbf{F}_i}{\sqrt{l_{ix}^2 + l_{iy}^2 + l_{iz}^2}} (l_{ix}, l_{iy}, l_{iz}). \quad (4)$$

By the equation (3) and (4), the coordinate (F_{i1}, F_{i2}, F_{i3}) can be written by

$$(F_{i1}, F_{i2}, F_{i3}) = \frac{\mathbf{F}_i}{\sqrt{l_{ix}^2 + l_{iy}^2 + l_{iz}^2}} (l_{ix}, l_{iy}, l_{iz}) \mathbf{T}^T. \quad (5)$$

4 Analysis for the platform dynamics

In order to analyze the platform dynamics, the motion of the platform is considered to be divided into two parts. The one is the translational motion and the other is the rotational motion. First, the translational motion of the platform is discussed.

4.1 Analysis for the translational motion

The equation for the translational motion of the centroid o' of the platform is represented

$$m \frac{d^2 \mathbf{R}}{dt^2} = \sum_{i=1}^6 \mathbf{F}_i + \mathbf{L} + \mathbf{M} \quad (6)$$

with respect to the fixed frame. By using the equation (4) which represents the components of the cylinder force vector relative to the base fixed frame, following three dynamical equations can be obtained.

$$\begin{aligned} m \frac{d^2 x}{dt^2} &= \sum_{i=1}^6 \frac{l_{ix}}{\sqrt{l_{ix}^2 + l_{iy}^2 + l_{iz}^2}} \mathbf{F}_i + L_x \\ m \frac{d^2 y}{dt^2} &= \sum_{i=1}^6 \frac{l_{iy}}{\sqrt{l_{ix}^2 + l_{iy}^2 + l_{iz}^2}} \mathbf{F}_i + L_y \\ m \frac{d^2 z}{dt^2} &= \sum_{i=1}^6 \frac{l_{iz}}{\sqrt{l_{ix}^2 + l_{iy}^2 + l_{iz}^2}} \mathbf{F}_i + L_z - mg \end{aligned} \quad (7)$$

4.2 Analysis for the rotational motion

Next, let us consider about the rotational motion of the platform. The equation for this motion is given

$$\frac{d\mathbf{H}}{dt} + \boldsymbol{\omega} \times \mathbf{H} = \sum_{i=1}^6 \mathbf{A}_{im} \times \mathbf{F} \quad (8)$$

with respect to the motion frame. $\boldsymbol{\omega}$ denotes the angular velocity vector for the platform and \mathbf{H} is an angular momentum vector. The $\boldsymbol{\omega}$ is

$$\begin{aligned} \boldsymbol{\omega} &= \omega_1 \mathbf{i} + \omega_2 \mathbf{j} + \omega_3 \mathbf{k} \\ &= \omega_1 \mathbf{i} + \omega_2 \mathbf{j} + \omega_3 \mathbf{k} \end{aligned} \quad (9)$$

with respect to the motion frame. Where, $\omega_1, \omega_2, \omega_3$ in (9) can be described with Euler angles ϕ, θ, ψ and these derivatives $\dot{\phi}, \dot{\theta}, \dot{\psi}$ as

$$\begin{aligned} \omega_1 &= \dot{\phi} - \dot{\psi} \sin \theta \\ \omega_2 &= \dot{\theta} \cos \phi + \dot{\psi} \cos \theta \sin \phi \\ \omega_3 &= -\dot{\theta} \sin \phi + \dot{\psi} \cos \theta \cos \phi \end{aligned} \quad (10)$$

The vector \mathbf{H} can be derived by

$$\mathbf{H} = \begin{bmatrix} H_1 \\ H_2 \\ H_3 \end{bmatrix} = \begin{bmatrix} I_{11} & I_{12} & I_{13} \\ I_{21} & I_{22} & I_{23} \\ I_{31} & I_{32} & I_{33} \end{bmatrix} \begin{bmatrix} \omega_1 \\ \omega_2 \\ \omega_3 \end{bmatrix}, \quad (11)$$

where $I_{ij} (i, j = 1, 2, 3)$ denotes the moment of inertia of the platform. Note that we considered the rotating frame of $\boldsymbol{\omega}$ as the motion frame which is fixed the platform and the square matrix for the inertia in eq (9) is diagonalizable and we obtain following equation

$$\mathbf{H} = \begin{bmatrix} H_1 \\ H_2 \\ H_3 \end{bmatrix} = \begin{bmatrix} I_{11} & 0 & 0 \\ 0 & I_{22} & 0 \\ 0 & 0 & I_{33} \end{bmatrix} \begin{bmatrix} \omega_1 \\ \omega_2 \\ \omega_3 \end{bmatrix}. \quad (12)$$

Therefore, the equation (8) can be rewritten as

$$\begin{aligned} \begin{bmatrix} \frac{dH_1}{dt} & \frac{dH_2}{dt} & \frac{dH_3}{dt} \end{bmatrix} \begin{bmatrix} \mathbf{i} \\ \mathbf{j} \\ \mathbf{k} \end{bmatrix} + \begin{bmatrix} \mathbf{i} & \mathbf{j} & \mathbf{k} \\ \omega_1 & \omega_2 & \omega_3 \\ H_1 & H_2 & H_3 \end{bmatrix} \\ = \sum_{i=1}^6 \begin{bmatrix} \mathbf{i} & \mathbf{j} & \mathbf{k} \\ a_{i1} & a_{i2} & a_{i3} \\ F_{i1} & F_{i2} & F_{i3} \end{bmatrix}. \end{aligned} \quad (13)$$

a_{i1}, a_{i2} and a_{i3} are the components of the vector \mathbf{A}_{im} which denotes attachment point of the cylinder on the platform relative to the motion frame. The elements for Equation (13) can be described as

$$\begin{aligned} I_1 \frac{d\omega_1}{dt} + (I_3 - I_2) \omega_2 \omega_3 &= \sum_{i=1}^6 (a_{i2} F_{i3} - a_{i3} F_{i2}) \\ I_2 \frac{d\omega_2}{dt} + (I_1 - I_3) \omega_3 \omega_1 &= \sum_{i=1}^6 (a_{i3} F_{i1} - a_{i1} F_{i3}) \\ I_3 \frac{d\omega_3}{dt} + (I_2 - I_1) \omega_1 \omega_2 &= \sum_{i=1}^6 (a_{i1} F_{i2} - a_{i2} F_{i1}). \end{aligned} \quad (14)$$

For above equations, let us rewrite F_{i1}, F_{i2} and F_{i3} to the cylinder force \mathbf{F}_i with the relations in equation (5), the following equations

$$\begin{aligned} I_1 \frac{d\omega_1}{dt} + (I_3 - I_2) \omega_2 \omega_3 &= \sum_{i=1}^6 \frac{a_{i2}(l_{ix} T_{31} + l_{iy} T_{32} + l_{iz} T_{33})}{\sqrt{l_{ix}^2 + l_{iy}^2 + l_{iz}^2}} \mathbf{F}_i \\ &\quad - \sum_{i=1}^6 \frac{a_{i3}(l_{ix} T_{21} + l_{iy} T_{22} + l_{iz} T_{23})}{\sqrt{l_{ix}^2 + l_{iy}^2 + l_{iz}^2}} \mathbf{F}_i \\ I_2 \frac{d\omega_2}{dt} + (I_1 - I_3) \omega_3 \omega_1 &= \sum_{i=1}^6 \frac{a_{i3}(l_{ix} T_{11} + l_{iy} T_{12} + l_{iz} T_{13})}{\sqrt{l_{ix}^2 + l_{iy}^2 + l_{iz}^2}} \mathbf{F}_i \\ &\quad - \sum_{i=1}^6 \frac{a_{i1}(l_{ix} T_{31} + l_{iy} T_{32} + l_{iz} T_{33})}{\sqrt{l_{ix}^2 + l_{iy}^2 + l_{iz}^2}} \mathbf{F}_i \\ I_3 \frac{d\omega_3}{dt} + (I_2 - I_1) \omega_1 \omega_2 &= \sum_{i=1}^6 \frac{a_{i1}(l_{ix} T_{21} + l_{iy} T_{22} + l_{iz} T_{23})}{\sqrt{l_{ix}^2 + l_{iy}^2 + l_{iz}^2}} \mathbf{F}_i \\ &\quad - \sum_{i=1}^6 \frac{a_{i3}(l_{ix} T_{11} + l_{iy} T_{12} + l_{iz} T_{13})}{\sqrt{l_{ix}^2 + l_{iy}^2 + l_{iz}^2}} \mathbf{F}_i \end{aligned} \quad (15)$$

can be obtained. $T_{ij}(i, j = 1, 2, 3)$ in equation (15) is the element of the oriental matrix \mathbf{T} .

Therefore, the dynamics of the 6DOF parallel manipulator can be described by six differential equations in equation (7) and (15).

5 Simulation

In this section, we provide the numerical simulation based on our analysis. Figure 4 shows the result for the surge motion (x direction) of the platform. Where, "cyl.1" denotes the 1st cylinder of the parallel manipulator. In Figure 4, the top diagram denotes the amount of the cylinder stretch and the bottom denotes the cylinder force amount for six cylinders. The lateral axis of both diagrams indicate the distance for the centroid o' of the platform. Figure 5 is the result for the yaw motion of the platform.

The trajectories for these motions are designed by using trigonometric function. The amplitude of the motion trajectory is 90mm and the frequency is 0.5Hz.

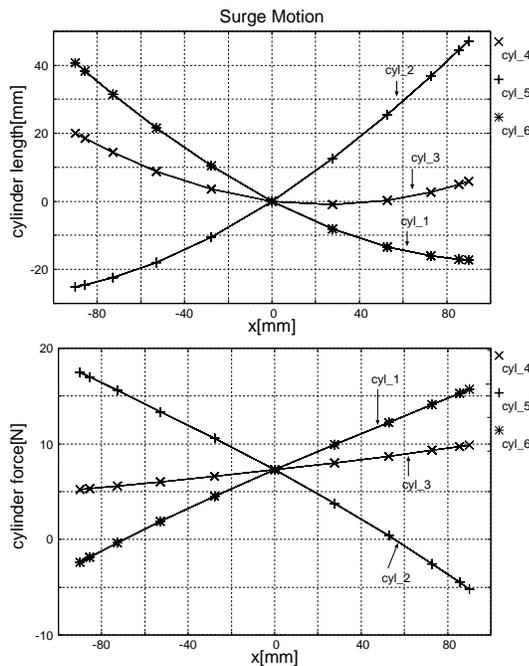


Figure 4: Results for surge motion

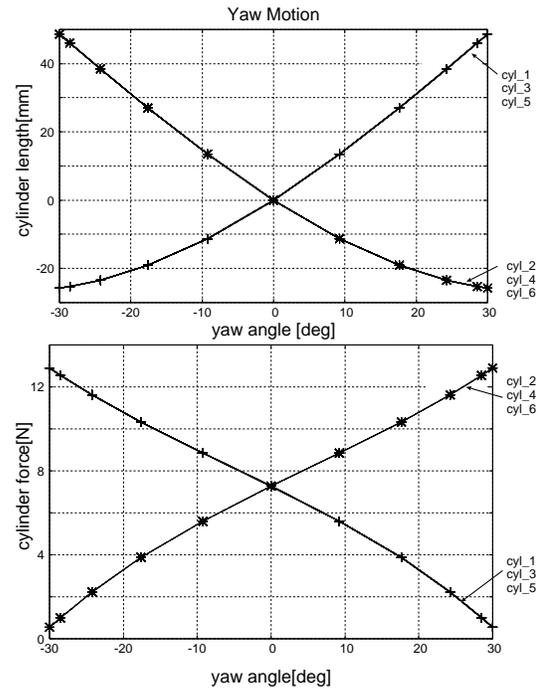


Figure 5: Results for yaw motion

6 Summary

In this paper, we analyzed the dynamics of the 6DOF parallel manipulator and showed the numerical simulation results.

In our future work, we'll confirm our analysis to compare with our simulation results and the experimental results for the actual parallel manipulator. And moreover, we'll utilize our analytical result to the force control for the parallel manipulator in order that the parallel manipulators can be useful in many fields such that the medical operation, high-precision processing technology and so on.

References

- [1] Stewart.D, A Platform with 6 degrees of freedom, Proc. Inst Mech. Eng, Vol.180, Part I, No15, pp.371-386, 1965-66.
- [2] K.H.Hunt, Structural Kinematics of In-Parallel-Actuated Robot-Arms, ASME, J.Mechanisms, Transmissions and Automation in Design, 105, (1983-12),705.